Observation of Second Sound in NaF by Means of Light Scattering

Dieter W. Pohl and V. Irniger
IBM Zurich Research Laboratory, 8803 Rüschlikon-ZH, Switzerland
(Received 15 December 1975)

Application of the technique of forced thermal light scattering allowed the observation of second sound in NaF in spite of the extremely weak coupling between light and thermal fluctuations. The velocity and damping were measured up to 23 K. These measurements extend the results of previous heat-pulse experiments in agreement with theory.

The observation of wavelike rather than diffusive propagation of heat pulses through ordinary crystals such as NaF[1,2] and Bi[3] recently renewed the interest in the phenomenon of second sound. The results of those heat-pulse experiments verified[4,5] theoretical work[6-10] which had been started almost thirty years ago.[11] However, they also made clear two serious shortcomings of this technique: (i) Excitation of monochromatic waves seems to be unfeasible; (ii) detection of second sound requires absorption lengths of the order of the sample dimensions. For these reasons the amount of information obtainable and the choice of crystals are quite restricted.

Light scattering of second sound will not suffer from the above problems. It can provide complementary and more detailed information.[12-15] It might also allow the detection of possibly existing heavily damped second sound in other materials. Classical light scattering, however, is not applicable for ordinary crystals because of the very unfavorable signal-to-noise ratio[16]: (i) The "window condition"[8] restricts the second-sound wavelength λ to values much larger than visible wavelengths for a material such as NaF (see below). Thus an extremely small scattering angle has to be chosen, which unavoidably will result in a high level of stray light at the detector. (ii) The coupling constant between light and thermal fluctuations gets extremely small at low temperatures, and the scattered intensity is correspondingly weak.[15,16]

The technique of forced thermal scattering (FTS) greatly improves the detectability of weak scattering processes.[17] The idea is to enhance artificially that particular Fourier component $\delta T(\vec{k}, \Omega)$ of the thermal fluctuation which is to be analyzed by means of light scattering. $\delta T(\vec{k}, \Omega)$ can be excited *in situ* by means of interference and absorption. A pair of intense amplitude-modulated pump light beams is brought to intersection inside the sample in such a way that sinusoidal intensity and temperature patterns are created [Fig. 1(a)]. An extension of the original FTS technique[17] enabled us to overcome the difficulties described above and observe "*second-sound scattering*" in NaF for the first time. Previously the modulation frequency $\Omega/2\pi$ of the pump light from a CO_2 laser was restricted to less than 3 kHz, i.e., $\Omega \simeq 0$. In the present experiment $\Omega/2\pi$ can be varied between 0 and 10 MHz. In this way it is possible to probe any resonance in the excitation spectrum of $\delta T(\vec{k}, \Omega)$ within this frequency interval.

The expected second-sound resonance comes about, briefly, as follows[18]: At low enough temperatures, thermal phonons interact predominantly via momentum-conserving normal processes, while momentum-destroying "resistive" umklapp (and impurity) processes become less frequent. In terms of the respective mean free paths λ_N and λ_R, the so-called *window* for second sound opens if $\lambda_N < \lambda = 2\pi/k < \lambda_R$. Consequently, the mean phonon flux $\vec{q}$ and the phonon density —felt as temperature $T = T_0 + \delta T$—not only con-

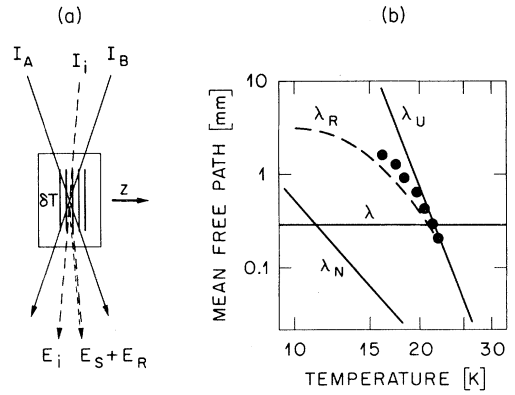

FIG. 1. (a) Principle of FTS. I_A and I_B are pump beams; E_i (I_i), E_S, and E_R are incident, scattered, and stray light beams (I and E refer to intensity and amplitude, respectively). (b) Mean-free-path diagram reconstructed from Ref. 4; circles, experimental damping lengths.

serve energy but also momentum:

$$C_v\dot{T} + \nabla \cdot \vec{q} = \alpha I_0 e^{i(\Omega t - kz)}, \quad (1)$$

$$\dot{\vec{q}} + (c/\lambda_R)\vec{q} + (C_v c^2/3)\nabla T = 0, \quad (2)$$

with the solution

$$\delta T(\vec{k}, \Omega) = \frac{(\alpha/C_v) I_0 (c/\lambda_R + i\Omega)}{(\frac{1}{3}c^2k^2 - \Omega^2 + i\Omega c/\lambda_R)}. \quad (3)$$

Equations (1)–(3) assume $\lambda_N \ll \lambda$. c and C_v are the velocity of first sound (TA) and the specific heat. The driving term in Eq. (1) is the absorbed (α) pump radiation of the two intersecting beams with intensities $I_A = I_B = I_0 \cos\Omega t$. The second-sound resonance occurs at $\Omega = c_{II}|\vec{k}|$, where c_{II} is equal to $c/\sqrt{3}$ if $\lambda_N \ll \lambda \ll \lambda_R$. The values of λ_R and λ_N, however, strongly depend on temperature. Figure 1(b) reproduces a mean-free-path diagram first constructed by Jackson and Walker.[4] The ratio of λ_R/λ_N is of the order of 10 to 100 only, and c_{II} therefore varies considerably with temperature.[1,2,4,5,19,20]

In the present experiment, we wished to operate well inside the window, and therefore adjusted the angle between the pump beams such that $\lambda = 295$ μm [36 mrad in air; $k = 213$ cm^{-1}; horizontal line in Fig. 1(b)]. A second-sound resonance then is expected between, say, 14 to 20 K and 6 to 7 MHz. The experimental apparatus is shown schematically in Fig. 2. A 100%-modulated variable-frequency pump wave (2–10 W) is obtained as the beat note of a pair of stabilized CO_2 lasers ($\lambda_L = 10.6$ μm).[21] The laser beams are superimposed at the Ge plate I and split up to form the pump beams A and B at plate II. The mirror

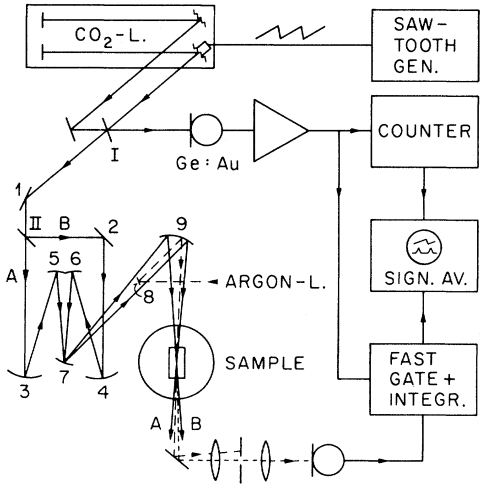

FIG. 2. Experimental setup.

system 2, ..., 7 serves to adjust independently the point of intersection in the sample, the angular separation, and the relative phase of beams A and B. The absorption of $\alpha \simeq 0.3$ cm^{-1} at 10.6 μm is caused by three-phonon processes.[22] The two beams generate a *standing* thermal pattern which consists of $\delta T(\vec{k}, \Omega)$ plus a static component $\delta T(\vec{k}, 0)$. The latter represents the Rayleigh peak and is useful for adjustment and calibration.

The NaF crystals were the same as in previous heat-pulse experiments.[1,2,4,5] Typical sample dimensions were $5 \times 5 \times 20$ mm^3. The samples were oriented in [100] directions and mounted on a cool finger in a He cryostat. The absorbed pump radiation raised the overall sample temperature to about 15 K; larger temperatures were attained by additional electric heating.

An argon laser ($\lambda_i = 0.5$ μm) was chosen for detection because the small wavelength increases the scattering efficiency, and the large intensity available improves the signal-to-noise ratio (signal $\sim |E_i|^2$; shot noise $\sim |E_i|$). After spatial filtering, the scattered light E_S together with a large amount of stray light $|E_R| \gg |E_S|$ falls onto a photomultiplier. The detected ac signal hence is proportional to $E_S E_R^*$. Random noise (mostly shot noise) from the stray light is eliminated effectively with a fast electronic gate activated by the CO_2-laser beat note. The high-frequency phase-sensitive detection achieved in this way greatly improves the recovery of the weak signal from noise. The signal is next fed into a signal averager which is synchronized with the slowly swept beat frequency. In this way, a display of $E_S E_R^*$ versus Ω is obtained. Integration times of up to 3 min were required for a clearly visible response. In some measurements, the pump radiation was chopped and the photomultiplier current was sent through an additional lock-in amplifier synchronized to the chopper frequency. Depending on the relative phase between E_S and E_R, either positive or negative signals were seen. Phase adjustment of $\delta T(\vec{k}, \Omega)$ by translation of mirror 4 allowed optimization of the signal with respect to E_R. However, the signal also depends on the phase between E_S and the gate pulse. The observed resonances, therefore, may deviate considerably from the approximately Lorentzian shape expressed by Eq. (3).

Figure 3 shows a number of typical signal-averager traces obtained from a sample cut out of Jackson and Walker's[2,5] purest crystal. Similar results were obtained with samples from McNelly *et al.*[1] No resonance could be resolved at 15 K

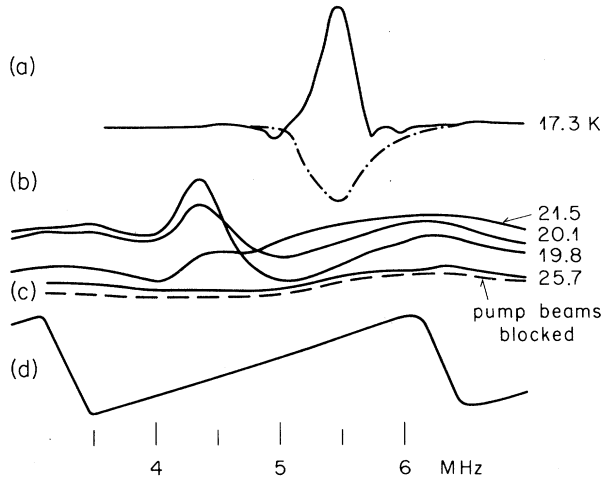

FIG. 3. Typical signal-averager traces.

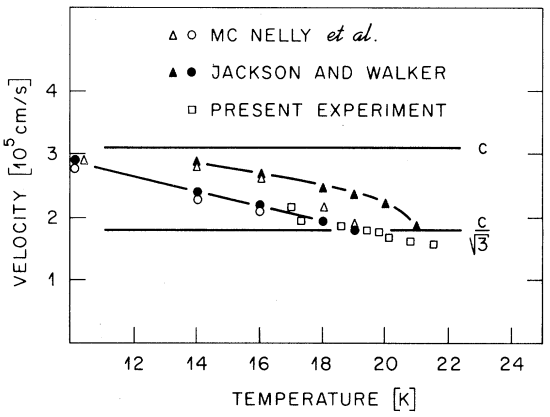

FIG. 4. First- and second-sound velocities in NaF. Triangles and circles refer to leading edges and peaks of heat pulses; squares refer to light scattering.

(probably because of a vanishing coupling constant). Above this temperature a signal rapidly rose out of noise and reached its maximum around 17 K (trace *a*). The demonstration of phase reversal (dash-dotted curve) upon translation of mirror 4 proves that $\delta T(\vec{k}, \Omega)$ is the origin of the resonance. With increasing temperature the peak gets smaller and broader (trace *b*). It finally transforms into a very wide and weak Rayleigh spectrum (trace *c*). Trace *d* is a control record of frequency $\Omega/2\pi$ versus time.

The signal-averager traces were fitted by Eq. (3) times a constant phase factor. The half-widths of the experimental peaks allow the determination of λ_R. The resistive mean free path is found to vary between 1.5 and 0.3 mm [circles in Fig. 1(b)]. These values compare favorably with the curves of the mean-free-path diagram. The peaks of the resonance shift towards lower frequencies with increasing temperature. The resulting speed of propagation Ω_{res}/k is plotted in Fig. 4 together with the velocity of second sound derived from heat-pulse experiments.[1,2,4,5] A perfect agreement is found which strongly supports our assignment. The data points are close to $c/\sqrt{3}$, indicating that temperature and wavelength of operation fit right into the center of the window. The increase above $c/\sqrt{3}$ at low temperatures is probably caused by incomplete thermalization[20] (λ_N too large). The decrease below $c/\sqrt{3}$ at higher T is a damping effect which can be accounted for quantitatively by the experimental values of λ_R. Above 20 K the damping length is considerably smaller than the sample dimensions. Under these circumstances second sound can no longer be seen by means of heat pulses. Light scattering, however, can still readily resolve the second-sound peak and follow the gradual transformation into the diffusive regime.

The present investigation greatly benefitted from the excellent NaF crystals made available to us by T. F. McNelly and H. E. Jackson. The authors gratefully acknowledge stimulating discussions with H. Beck, C. P. Enz, and P. F. Meier on second sound, and with C. Freed and A. Szöke on laser-design problems. They wish to thank E. Courtens for careful reading of the manuscript.

[1]T. F. McNelly, S. J. Rogers, D. J. Channin, R. J. Rollefson, W. M. Goubeau, G. E. Schmidt, J. A. Krumhansl, and R. O. Pohl, Phys. Rev. Lett. 24, 100 (1970).

[2]H. E. Jackson, C. T. Walker, and T. F. McNelly, Phys. Rev. Lett. 25, 26 (1970).

[3]V. Narayanamurti and R. C. Dynes, Phys. Rev. Lett. 28, 1461 (1972).

[4]H. E. Jackson and C. T. Walker, Phys. Rev. B 3, 1428 (1971).

[5]S. J. Rogers, Phys. Rev. B 3, 1440 (1971).

[6]J. C. Ward and J. Wilks, Philos. Mag. 42, 314 (1951).

[7]M. Chester, Phys. Rev. 131, 2013 (1963).

[8]E. W. Prohofsky and J. A. Krumhansl, Phys. Rev. 133, A1411 (1964); R. A. Guyer and J. A. Krumhansl 148, 766, 778 (1966).

[9]C. P. Enz, Ann. Phys. (N.Y.) 46, 114 (1968).

[10]H. Beck, P. F. Meier, and A. Thellung, Phys. Status Solidi (a) 24, 11 (1974).

[11]V. Peshkow, in *Proceedings of the International Conference on Fundamental Particles and Low Temperatures, Cambridge, 1946* (The Physical Society, London, 1947), p. 19.

[12]A. Griffin, Phys. Lett. 17, 208 (1965), and Rev. Mod. Phys. 40, 167 (1968).
[13]R. A. Guyer, Phys. Lett. 19, 261 (1965).
[14]R. H. Enns and R. R. Haering, Phys. Lett. 21, 534 (1966).
[15]R. K. Wehner and R. Klein, Physica (Utrecht) 62, 161 (1972).
[16]D. W. Pohl and S. E. Schwarz, Phys. Rev. B 7, 2735 (1973).
[17]D. W. Pohl, S. E. Schwarz, and V. Irniger, Phys. Rev. Lett. 31, 32 (1973).
[18]Excellent derivations of the second-sound equations can be found in Refs. 6–10; the present expressions were first used by Chester (Ref. 7).
[19]R. J. Hardy and S. S. Jaswal, Phys. Rev. B 3, 4385 (1971).
[20]H. Beck, Z. Phys. B 21, 209 (1975).
[21]This technique turned out to be by far more efficient than electro-optic modulation which does not easily provide large modulation and tunability simultaneously.
[22]D. W. Pohl and P. F. Meier, Phys. Rev. Lett. 32, 58 (1974); D. W. Pohl and T. F. McNelly, Phys. Rev. Lett. 32, 1305 (1974).

Operator Identity and Applications to Models of Interacting Electrons

Daniel C. Mattis
Belfer Graduate School of Science, Yeshiva University, New York, New York 10033
(Received 21 July 1975)

By correct reduction of some quartic forms in fermion field operators, I eliminate all but a constant and some quadratic terms. I can use this to transform the Wolff model, of a magnetic impurity in a nonmagnetic metal, into a solvable quadratic form in fermions. Applying the same method (with less justification) to Hubbard's model in three dimensions, I obtain an oversimplified but nevertheless suggestive, and diagonal, Hamiltonian.

In this paper I present elements of a novel solution of a well-known model magnetic impurity in a nonmagnetic metal, first proposed by Wolff.[1] In an earlier study Tomonaga's method[2] was used to reduce this many-body problem to a solvable quadratic form in boson operators.[3] I have now transformed it further, into an exactly solvable quadratic form in fermion operators, by a method detailed below. Like the old, the new method indicates that there is a singularity at a value of the Coulomb parameter U_C of the order of the bandwidth, but unlike the old[4] it can provide detailed results in the critical region $U \approx U_C$ replete with symptoms of the Kondo effect: specific-heat anomaly, high magnetic susceptibility, low-frequency resonance which can translate into a resistance anomaly. Finally, an approximate extension of this method to Hubbard's model[5] of an interacting electron gas yields as the solution of that problem a simple, diagonal, yet physically plausible Hamiltonian.

I recapitulate parts of my earlier study.[3] The interaction between electrons of opposite spin σ at the impurity site $R_i = 0$ is given by

$$\mathcal{H}_2 = U[n_\uparrow(0) - \tfrac{1}{2}][n_\downarrow(0) - \tfrac{1}{2}]$$
$$= \tfrac{1}{4}U\{[n_\uparrow(0) + n_\downarrow(0) - 1]^2 - [n_\uparrow(0) - n_\downarrow(0)]^2\}. \quad (1)$$

The dual representations of the local occupation-number operator are

$$n_\sigma(0) - \tfrac{1}{2} = N^{-1}\sum_k \sum_{k' \neq k} c_{k\sigma}^\dagger c_{k'\sigma}, \quad (2a)$$

which is quadratic in the fermion field operators c_k, and

$$n_\sigma(0) - \tfrac{1}{2} = N^{-1}\sum_{q>0}(\rho_{q\sigma} + \rho_{q\sigma}^\dagger),$$
$$\rho_{q\sigma} = \rho_{-q\sigma}^\dagger = \sum_k c_{k\sigma}^\dagger c_{k+q,\sigma}, \quad (2b)$$

which is linear in the bosons. Momentary reflection suggests that $\mathcal{H}_2$, expressed in bosons, will become separable after a unitary transformation to new operators denoted $\rho_{q\tau} \equiv 2^{-1/2}(\rho_{q\uparrow} + \tau\rho_{q\downarrow})$, where $\tau = \pm 1$. The "kinetic energy" operator $\mathcal{H}_0$ of a half-filled band is invariant under such transformation. Originally there are two equivalent forms:

$$\mathcal{H}_0 = \sum_{k,\sigma} \epsilon_k c_{k\sigma}^\dagger c_{k\sigma}, \quad \epsilon_k = v_F(k - k_F), \quad (3a)$$

in the original fermions, or

$$\mathcal{H}_0 = 2\pi v_F N^{-1} \sum_{q>0,\sigma} \rho_{q\sigma}^\dagger \rho_{q\sigma}, \quad (3b)$$

in the original bosons. After transformation to the new operators, $\rho_{q\tau}$, this last equation be-